Journal of Archaeological Science 40 (2013) 1176–1185

Contents lists available at SciVerse ScienceDirect

Journal of Archaeological Science

journal homepage: http://www.elsevier.com/locate/jas

Thermoluminescence dates for the Middle Palaeolithic site of Chez-Pinaud Jonzac (France)

Daniel Richter [a,b,*], Jean-Jacques Hublin [a], Jacques Jaubert [c], Shannon P. McPherron [a], Marie Soressi [a,d], Jean-Pierre Texier [c]

[a] Department of Human Evolution, Max Planck Institute for Evolutionary Anthropology, Deutscher Platz 6, 04103 Leipzig, Germany
[b] Lehrstuhl Geomorphologie, University of Bayreuth, Universitätsstraße 30, 95447 Bayreuth, Germany
[c] University of Bordeaux1, PACEA UMR 5199 (CNRS UB1 MCC), Bordeaux, France
[d] INRAP, 45590 St Cyr-en-Val, France

ARTICLE INFO

Article history:
Received 25 May 2012
Received in revised form
28 August 2012
Accepted 1 September 2012

Keywords:
Thermoluminescence dating
Middle Palaeolithic
Quina Mousterian
Mousterian of Acheulean Tradition
MTA
Chez-Pinaud Jonzac

ABSTRACT

Thermoluminescence dating of heated flint artefacts from the Middle Palaeolithic sequence of Chez-Pinaud Jonzac (France) places an assemblage of Quina type Mousterian into MIS 4, while the overlying assemblage of Denticulate Mousterian which is followed by two layers with Mousterian of Acheulean Tradition are all assigned to MIS 3. TL dating is used to verify the mixed nature of deposits from which diagnostic Middle as well as Upper Palaeolithic tools were recovered. The TL ages are significantly different for samples from this layer and broadly agree with the archaeological attributions. While the study is generally limited by the low number of heated samples available, a correlation with a generalized chronostratigraphic sequence is possible by including proxy data from the faunal remains associated with the lithic assemblages in question. The Quina Mousterian in southwestern France, therefore, can be placed by chronometric dating methods in MIS 4 to MIS 3.

1. Introduction

The site of Chez Pinaud Jonzac (hereafter Jonzac) is a collapsed rock shelter situated in the Seugne River valley in the Charente-Maritime department of southwest France (Fig. 1). The site was first recognized by the geologist Marchais in 1997 and subsequently excavated by Airvaux between 1998 and 2003 (Airvaux et al., 2004; Airvaux and Soressi, 2005). This work established that the site had a deep sequence of Late Middle Palaeolithic industries capped by a thick deposit of mostly sterile sediments that include some dispersed Early Upper Palaeolithic lithics. An effort to date these deposits by AMS and TL was unsuccessful (Airvaux, 2004), thus from 2004 to 2007 a new series of excavations was conducted at the site (Jaubert et al., 2008, Jaubert et al., 2010) in part to re-attempt a dating of the sequence (Britton et al., 2011; Niven et al., 2012; Richards et al., 2008). This dating effort includes AMS radiocarbon dating of bones from the upper Middle Palaeolithic levels (Jaubert et al., 2008), OSL (work in process) and Thermoluminescence (TL) dating of heated flints.

The results of the latter are reported here and the chronometric data is placed in a chronostratigraphical framework, with Marine Isotope Stages (MIS) as a general reference. However, direct correlation of terrestrial and marine sequences can be problematic (e.g. Sanchez Goni et al., 2000), sometimes delayed (e.g. Sier et al., 2011) and the terrestrial record appears to be more complex in some instances (e.g. Guiter et al., 2003), while certainly being comparable on a larger scale (e.g. Orombelli et al., 2010). However, studies of proxy data from close by sites in Western Europe, like lake Les Echets (e.g. Wohlfarth et al., 2008) and a speleothem from Villars Cave (e.g. Genty et al., 2010) indicate good correlation between marine and terrestrial proxies and reference is therefore made to MIS here, in order to attribute more precise age estimates through the combination of chronometric ages with proxy data available. TL ages are traditionally provided with an uncertainty of 68% (1-σ) and need to double (2-σ) in order to have sufficient confidence (95%) that the true age actually lies within the probability range given. It is only within 2-σ that any chronometric age should be interpreted when it is compared to other data, whether chronometric or proxy (e.g. Richter, 2007). The 2-σ age ranges therefore often allow the nominal attribution to more than one MIS

* Corresponding author. Department of Human Evolution, Max Planck Institute for Evolutionary Anthropology, Deutscher Platz 6, 04103 Leipzig, Germany. Tel.: +49 (0) 341 3550354.
E-mail address: drichter@eva.mpg.de (D. Richter).

0305-4403/$ – see front matter © 2012 Elsevier Ltd. All rights reserved.
http://dx.doi.org/10.1016/j.jas.2012.09.003

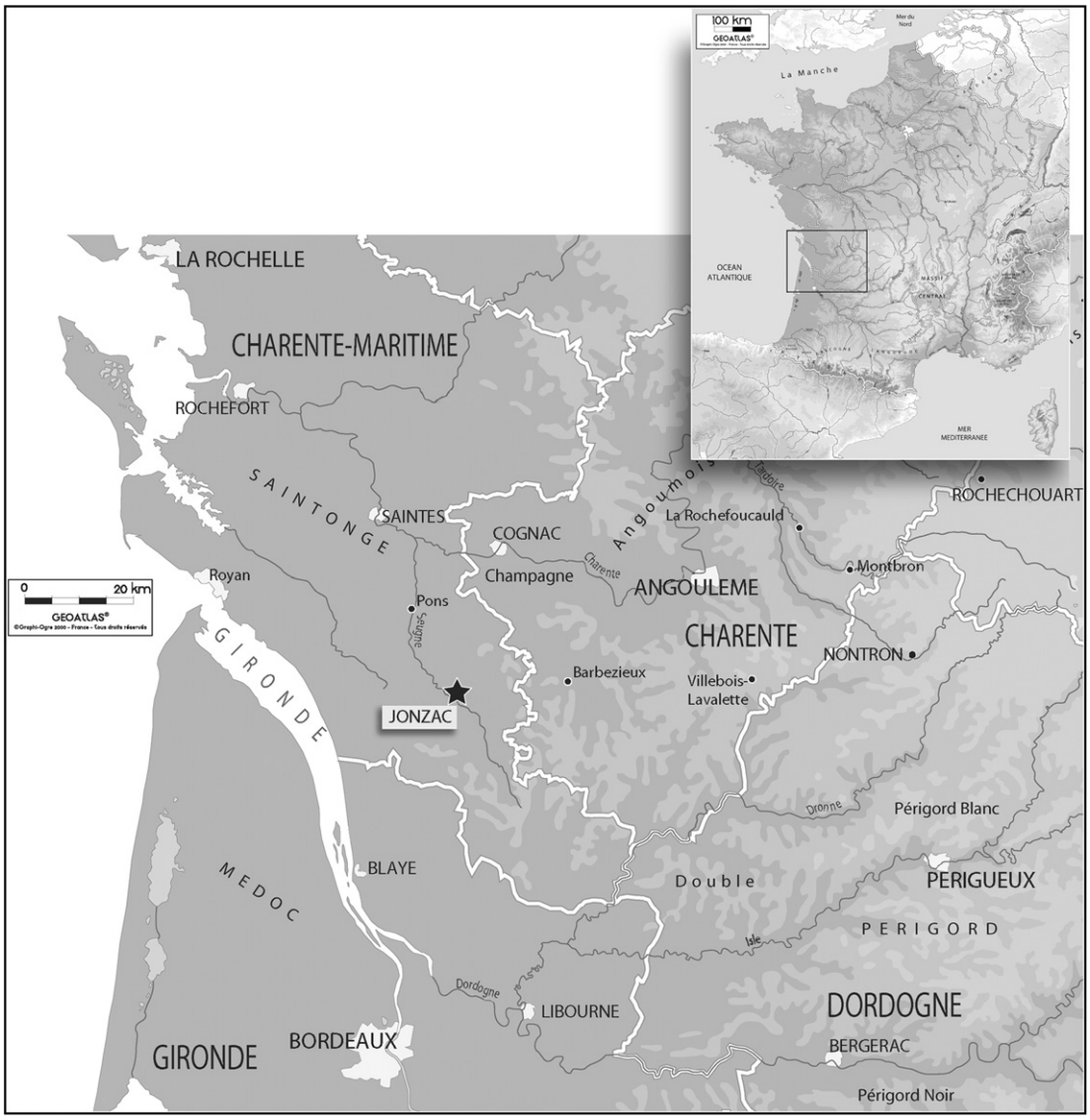

Fig. 1. Location of Jonzac in SW-France.

or substage, while proxy data might provide a more precise attribution within the chronometric age range and thus the most parsimonious age.

2. Stratigraphy, lithics and fauna of the Middle Palaeolithic sequence of Chez-Pinaud Jonzac

The site is situated against a low limestone cliff face in the broad valley of the Seugne River, which is tributary to the Charente River. Starting in the 19th century, the limestone at this site was exploited and a road was cut through the gently sloping valley deposits to gain access to the cliff face. This road exposed a section which was recognized in 1997 and then excavated by Jean Airvaux (2004). These and the subsequent excavations mainly consisted of a rectification of the steeply sloping sediments that form the road cut. The work resulted in one east and one west section, separated by the road. Excavations of both projects have mainly concentrated on the west section, though some testing of the sequence on the east section was also conducted.

Airvaux recognized 24 layers defined primarily on the basis of archaeological criteria (Fig. 2). One feature of the sequence is the presence of sterile sediments separating archaeological find horizons. In general, Airvaux used even numbers to denominate layers with archaeological finds and odd numbers to denominate the intervening sterile layers. The subsequent excavations followed Airvaux's system with only the addition of some sublevels, particularly in the thicker archaeological deposits at the base of the sequence. Thus, the numeric portion of the layer names reported here is strictly correlated with those already reported by Airvaux (2004) and Airvaux and Soressi (2005). However, a designation was added to each layer indicating the section of the site in which they were excavated (E = East, SW = South-West, and W = West) as well as the prefix US (*unité stratigraphique*). Even though the west and southwest sections were stratigraphically connected during the course of the excavation, the SW designation is retained here in order to provide continuity with previous publications (Fig. 3). However, the east and west sections are not connected stratigraphically and while the two sequences are overall similar, individual layer numbers are not necessarily strictly correlated.

The archaeological sequence is contained in deposits that have been divided lithostratigraphically into five geological units (Texier in Jaubert et al., 2008, p. 211). The lowest most layers (24–9/unit 5)

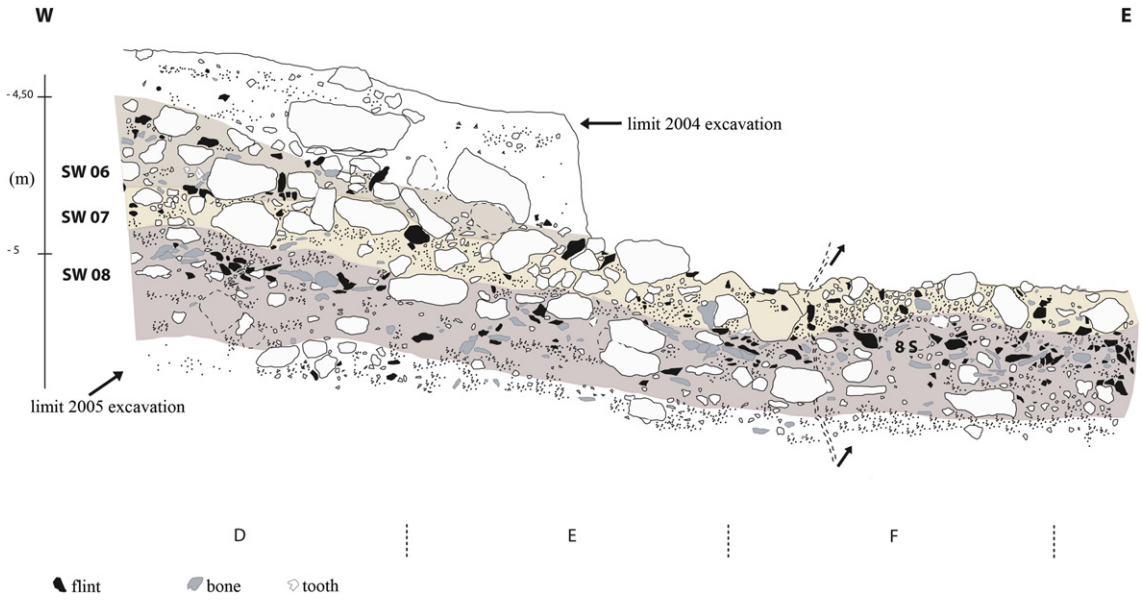

Fig. 2. Profile of the SW-section (line 8/10) of Jonzac from the recent excavation (2005 drawing D. F. Berrouet, CAD É. Boche).

are located in a deposit of yellow–brown, clayey sands with no evidence of soil formation and with little evidence of stratification except for some more sandy lenses localized against the cliff face. The sediments of this unit were likely deposited by water in combination with solifluction. However, these processes did not substantially alter the archaeological deposits because Layer W-US22 contained several instance of faunal elements in anatomical connection (Niven et al., 2012), the artefacts and bone were not strongly re-aligned (Jaubert et al., 2008), and a concentrated pile of lithic debris with refits was found in the layer. Layer SW-US8 to SW-US6 (unit 4) are dark brown sandy clay units, characterized by rounded limestone blocks/gravel and sometimes quartz gravels. Here the blocks but also the artefacts are more strongly oriented with the slope of the deposit than in the underlying layers. In addition to the more poorly preserved fauna, the lithics also show higher rates of edge damage. The depositional environment is also one of water and solifluction; however, in this case, particularly in Layers SW-US7 and SW-US6, the effects on the archaeology are more pronounced than in the underlying unit. In these later levels it is clear that there has been some downslope displacement of the artefacts of an unknown distance. Units 3–1 are archaeologically sterile or contain only few artefacts.

The Jonzac excavations have not reached the underlying bedrock, but coring indicates several more metres of sediment, including alluvial sediments above the substrate. The base of the excavated deposit is characterized first by a thick (~1.5 m), very well preserved, bone bed deposit (Layers 24–22) associated with Quina Mousterian, followed by a series of thin, archaeological layers (Layers 20–9) with high bone densities and Quina type industries separate from one another by thicker sterile deposits. For Layer W-US22 a surface of just under 8 m^2 was excavated to a depth of 30 cm, with some limited excavation of Layers 20–9. With Layer

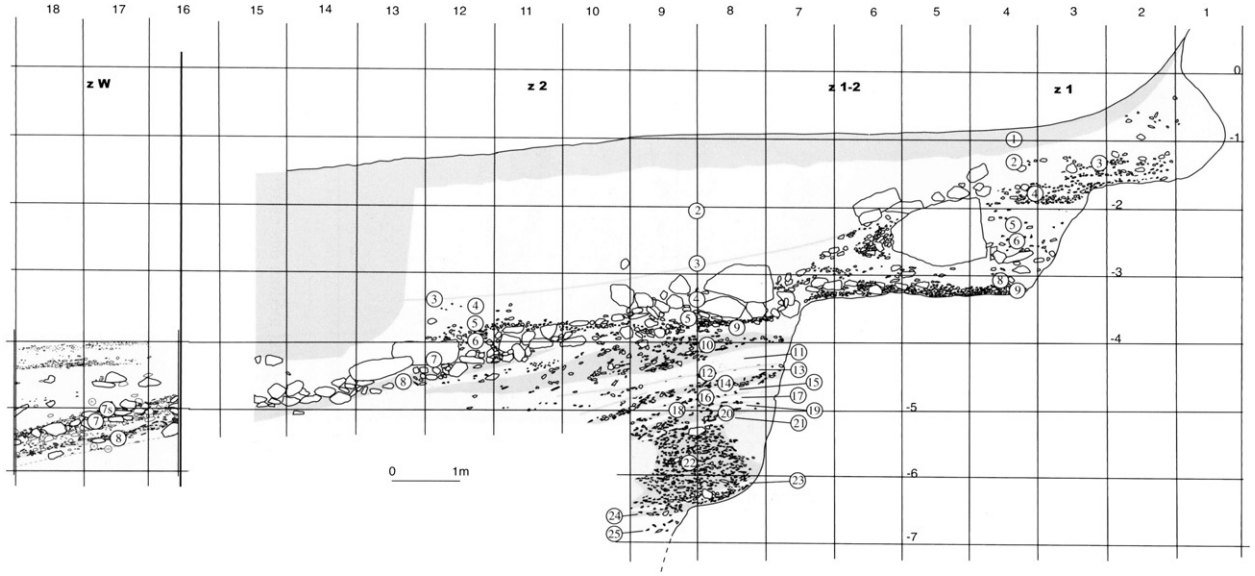

Fig. 3. Profile from the main section (from Airvaux and Soressi, 2005).

SW-US8 the sequence changes abruptly. This layer is extremely rich in lithics with a poorly preserved fauna. The lithics are typologically a Denticulate Mousterian on a Levallois technology. The reported presence of a Châtelperronian industry in Layer 8 (Airvaux and Leveque, 2004) can not be confirmed for the more recent sample from the sequence. The overlying deposit containing similar archaeological material is subdivided into two layers (SW-US7 and SW-US6) based primarily on the presence (in Layer SW-US6) of limestone blocks that represent the collapse and retreat of the shelter. Bone preservation continues to be poor in these levels. The lithic technology changes to Mousterian of Acheulian Tradition (MTA) with characteristic bifaces, notched tools, and backed knives and with a technology of blank production that includes some Levallois and some discoidal. Overlying the MTA are deposits with virtually no bone preservation and very low density, highly dispersed lithics. These lithics, where identifiable, appear to be Aurignacian (Jaubert et al., 2008).

The rich and well preserved fauna of the Quina layers (Layers 24–9) is dominated by reindeer (*Rangifer tarandus* 73–87%), with horse and large bovids, as well as rhino and hare being present, pointing more towards a cold, dry and open environment (Niven et al., 2012). The bone surface preservation is good with little evidence of carnivore impact, and a substantial number of bones show human impact (marrow exploitation patterns) and cut-marks (10–27%). The fauna from the MTA and Denticulate Levallois layers (SW-US06 to SW-US08) is dominated by large bovids (*Bos*/*Bison*), with reindeer and horse (*Equus* sp.) being abundant and some giant and red deer, as well as lion and bear. Little evidence of carnivore impact has to be noted and cutmark frequency is 3% in these faunal assemblages, which are indicating temperate and moist, but more closed habitats. Such data is consistent with the climate change from MIS 4 to MIS 3, however, it could also represent changes in subsistence strategies and other proxy data are required.

3. Chronostratigraphic position of the Jonzac sequence

Whether particular types of the traditionally recognized Mousterian 'facies' (e.g. MTA, Denticulate Mousterian, etc.) represent discrete time intervals (Mellars, 1965, 1969, 1996), or whether some or all of the Mousterian facies overlap in time, has been debated for decades. A recent summary of the available dates (Guibert et al., 2008) shows that at least the classical MTA, Quina and Denticulate type Mousterian chronologically overlap, which is supported in other studies and for other facies (Richter et al., 2012). However, stratigraphically, as is the case at Jonzac, at least the MTA typically occurs late in Middle Palaeolithic sequences and is overlying the Quina Mousterian (Jaubert et al., 2011; Mellars, 1969).

Based on the small set of available chronometric data, Guibert et al. (2008) suggest an age range of approximately 54–39 ka (MIS 3 to the end of the Middle Palaeolithic) for the Quina Mousterian, fully overlapping with the MTA. A survey of fauna associated with the Quina Mousterian (Delpech, 1996; Discamps et al., 2011) shows it to be always reindeer dominated in the Charente and Perigord regions, as is the case at Jonzac, which is just southwest of the Charente. Discamps et al. (2011) suggest that the Quina might start around Heinrich event 6 or late MIS 4 and continue only until early MIS 3. Currently the oldest chronometric date for an assemblage containing bifaces and generally attributed to the MTA is the weighted mean age of 64.6 ± 3.1 ka for burnt sediment from a combustion feature in Layer C of the Grotte XVI (Guibert et al., 1999), but most of the dates appear to cluster between 55 and 40 ka at the end of the Middle Palaeolithic in the first half of MIS 3. Recently obtained ^{14}C-AMS and TL dates for the MTA portion of Pech de l'Aze IV (McPherron et al., 2012; Richter et al., 2012) also fall within this time period.

Three bones from the Jonzac sequence have been AMS radiocarbon dated (Jaubert et al., 2008). The two radiocarbon dates for the Middle Palaeolithic MTA Layers SW-US6 and SW-US7 are at the upper limit of the age range usually given for the MTA of 70–39 ka (Guibert et al., 2008; Soressi et al., 2007) and place the MTA of Jonzac in the same time frame as e.g. the TL-date of 36.3 ± 2.7 ka for the Châtelperronian of nearby Saint-Cesaire (Mercier et al., 1991) and of 37.18 ± 0.42 ka for the Proto-Aurignacian of Isturitz (Szmidt et al., 2010). However, we consider these ages as preliminary, because the collagen yields were low, and a new set of AMS radiocarbon ages for the upper part of the Jonzac sequence is in progress. The preliminary TL ages for the sequence as reported by Jaubert et al. (2008) are superseded by the results presented here.

4. Thermoluminescence dating of heated flint from Jonzac

Thermoluminescence (TL) dating of heated flint artefacts determines the timing of the last heating of rock material, and thus the time elapsed since the prehistoric human activity of lighting a fire. It is one of the few instances where chronometric dating can provide an age estimate of a prehistoric activity directly (Richter, 2007) and the association of the sample and the event dated is secured (Dean, 1978).

The method of TL dating of heated flint artefacts is based on the accumulation of metastable charges (palaeodose) in the crystal lattice by ionizing radiation since the last heating of the rock (Aitken, 1985). Such charges in the crystal lattice of minerals are caused by the ionizing radiation due to the decay of radioactive elements from the surrounding sediment (external dose) and the sample itself (internal dose), as well as secondary cosmic rays (external dose). This omnipresent ionization causes a radiation dose (palaeodose or P) to accumulate in the crystal in the form of electrons in excited states. For dating application only electrons in metastable states are targeted, which are resident over periods of time much longer (approximately 50 Ma after Wintle and Aitken, 1977) than the anticipated age. The ratio of accumulated dose (palaeodose) to the sum of a series of dose rates (external and internal) provides the age of the last eating. Detailed descriptions of the principles of luminescence dating methods can be found elsewhere (Aitken, 1985, 1998; Botter-Jensen et al., 2003; Wagner, 1998) and a general account of TL dating of lithics is given in Richter (2007).

4.1. Methods

Artefacts showing macroscopic traces of heating, like potlids, craquelation, crenation, reddening (Richter, 2007), were submitted for TL-analysis. The majority is not suited for TL dating because temperatures achieved were too low to allow TL dating. Only samples passing the heating plateau test (after Aitken, 1985) which provides an indication for the complete zeroing, and thus fulfilling a basic assumption, were analysed (see Supplementary material for details).

Because the UV-blue luminescence signal of the samples from Jonzac is well within the linear dose range, the palaeodose on the 90–160 μm fractions of the crushed flint material (after the removal of the outer 2 mm) was obtained by a multi-aliquot-additive-regeneration (MAAR) protocol (Aitken, 1985). The integration range of all luminescence signals analysed was defined by the range of overlap of the temperature ranges of the heating plateau with the equivalent dose plateau in order to achieve the most accurate and precise results. A more detailed description of the procedures used is given in the electronic supplement.

4.2. Dosimetry

Of major concern in dosimetric dating is the assumption of the constancy of the dose rates over burial time and its spatial homogeneity. The former is certainly valid for the internal dose rate of the heated flints because only unaltered parts are used (i.e. not patinated). Only samples lacking macroscopic grain size variation, veins, etc., were selected, in order to minimize inhomogeneity effects (potentially leading to spatial differences in dose rates), which are usually related to macroscopically visible difference (e.g. Schmidt et al., 2012). The assumption of the constancy of the external dose rates (i.e. external γ only, in the case of flints) has to be verified by HpGe γ-spectrometry. But, only the present state can be determined and past changes (i.e. disequilibrium in the decay chains of Th and U) are difficult to detect and to model, especially as they could have occurred repeatedly. Because of size limitations only the smaller sediment particles can be analysed in the laboratory by HpGe γ-spectrometry (i.e. rocks and larger artefacts are not included, but bone fragments were). The results for γ-dose rates are therefore not necessarily representative if the sediment contains abundant rocks and artefacts ('lumpy' after Schwarcz, 1994). HpGe γ-spectrometry (50% SiO_2 + 50% $CaCO_3$ matrix) was therefore used only for the verification of the constancy of the external γ-dose rate from these sediments, which consist mainly of rock debris from cliff erosion with clay. External γ-dose rates are obviously not spatially homogeneous in such cases. Therefore, the external γ-dosimetry has to be either reconstructed and modelled (e.g. Guerin, 2012; Guibert et al., 1998), or measured with dosemeters which are small enough to be placed in positions/geometries similar to the ones occupied by the sample. Here, the external γ-dose rates used for age calculations are based on α-Al_2O_3:C-dosemeter measurements, employing the method described by Richter et al. (2010). The dosemeters were inserted in as many as possible locations into the sediment profiles for the duration of one year and were therefore exposed to the present day seasonal changes in sediment moisture. The present day moisture was assumed to best represent the average past conditions, especially as it would be difficult to calculate or model any past moisture contents. Because dosemeters were placed after every season of excavation, many different geometries of these sediments could be measured. From the dosimetric point of view the sediments are considered very 'lumpy' (Schwarcz, 1994) with varying degrees of rubble and boulders from the limestone cliff, which are incorporated in the clayey sediments. The lithic artefacts sampled for dating originate from a variety of geometries within the sediments, and were thus potentially exposed to different external γ-dose rates (e.g. in clay pockets versus next to large rocks). Obviously, precise and accurate γ-dose rate measurements are not possible for each sample in such cases. Using the nearest dosemeter value is a questionable approach because it might not have been exposed in the exact same geometry (i.e. volumes of sediment and rocks within the ~60 cm diameter sphere of the gamma radiation in relation to the distance to the sample) if the sediments contain larger pieces of rocks, as is the case here. The averaged gamma dosimetry from a number of positions for dosemeters for a given layer is therefore used. As the geometry of such positions at a depth of 30 cm can not be determined a priori the dosemeter positions can be considered as random positions, which are roughly equal the positions, and thus geometries, of the samples dated, which are not known to a sufficient extend either. As a consequence none of the samples age is calculated with the true external γ-dose rate.

By having to employ an average value for the external γ-dose rate, the variance of age results for a given layer is generally increased, because of the different proportional contribution of the external γ-dose rate to the total dose rate, and is likely larger than the variance of dosemeter results. This applies to any dosimetric dating method of objects. However, under the assumption that the last heating of the samples took place at roughly the same time, the mean of the age results based on the mean dosemeter readings will provide a good approximation for the time of the last heating of the samples from a layer or context. For 'lumpy' sites only age determinations with TL on large numbers of sample as well as dosemeters can be considered as representing an estimate close to the true mean, unless the geometry can be modelled/measured to a sufficient extend. Of course the availability of profiles and samples causes restrictions to the approach and sample numbers can potentially be used as an indicator of the robusticity of results.

Table 1
Location of samples used for TL analysis and Neutron Activation results.

EVA-LUM number	Area/layer	Square	Inv.-no.	*x* (m)	*y* (m)	*z* (m)	U (ppm)	Th (ppm)	K (ppm)
06/35	E-US05.2	L14	31	1012.047	1086.934	−4.148	1.15 ± 0.07	0.64 ± 0.04	1020 ± 286
05/20	E-US05.2	L16	12	1012.219	1084.715	−4.393	0.50 ± 0.05	0.41 ± 0.04	702 ± 288
06/30	E-US05.2	L16	6	1012.613	1084.957	−4.305	0.40 ± 0.05	0.54 ± 0.04	303 ± 24
07/40	E-US05.2	K13	8	1011.963	1087.617	−4.087	0.55 ± 0.07	1.99 ± 0.08	655 ± 524
06/36	E-US05.2	L16	38	1012.454	1084.347	−4.504	0.38 ± 0.04	0.46 ± 0.10	559 ± 15
06/37	E-US06.1	L14	112	1012.622	1086.114	−4.588	0.73 ± 0.04	0.18 ± 0.03	286 ± 8
05/21	SW-US06.1	D16	218	1004.512	1084.562	−4.867	0.60 ± 0.10	0.32 ± 0.07	3010 ± 1054
07/41	SW-US06.1	D19	240	1004.795	1081.295	−5.524	0.39 ± 0.05	0.21 ± 0.02	445 ± 32
08/23	SW-US06.3	D19	721	1004.827	1081.632	−5.724	0.36 ± 0.06	0.28 ± 0.04	426 ± 22
07/42	SW-US07	F15	151	1006.333	1085.520	−5.141	0.36 ± 0.03	0.17 ± 0.03	278 ± 9
07/43	SW-US07	E14	580	1005.788	1086.768	−4.686	0.36 ± 0.01	0.23 ± 0.02	347 ± 13
06/31	SW-US08	F16	212	1006.190	1084.660	−5.440	0.80 ± 0.07	0.22 ± 0.04	2000 ± 420
06/32	SW-US08	E16	830	1005.477	1084.739	−5.217	0.53 ± 0.01	0.17 ± 0.03	703 ± 260
06/33	SW-US08	K12	329	1011.588	1088.461	−4.533	0.83 ± 0.06	0.52 ± 0.03	1180 ± 425
07/44	SW-US08	D16	1977	1004.586	1084.558	−5.257	0.62 ± 0.04	0.31 ± 0.04	334 ± 11
06/34	SW-US08	D16	1417	1004.680	1084.810	−5.142	0.53 ± 0.03	0.33 ± 0.04	448 ± 15
07/45	SW-US08	F13	236	1006.218	1087.220	−4.805	0.46 ± 0.03	0.23 ± 0.03	370 ± 12
06/38	SW-US08	E16	1743	1005.569	1084.751	−5.379	0.46 ± 0.02	0.21 ± 0.02	446 ± 14
07/46	SW-US08	G16	411	1007.274	1084.654	−5.509	0.33 ± 0.04	0.31 ± 0.02	918 ± 42
08/24	SW-US08	F15	580	1006.015	1085.964	−5.097	0.92 ± 0.07	0.38 ± 0.03	395 ± 20
07/47	W-US022.1	G10	551	1007.645	1090.851	−5.627	0.77 ± 0.04	0.32 ± 0.04	460 ± 14
08/25	W-US22	F10	568	1006.826	1090.892	−5.660	0.36 ± 0.05	0.12 ± 0.02	308 ± 27
08/26	W-US022.2	H8	334	1008.021	1092.833	−5.583	0.13 ± 0.10	0.10 ± 0.05	57 ± 9

The specified sub-layers at Jonzac represent changes in sedimentation, which can not be necessarily linked to environmental changes or different human occupations. The dosimetry can not be measured individually and the sub-layers are combined for lithic analysis as well as for dating. This assumption is supported by the similarity of the sediment and homogeneity of the lithic inventory. Furthermore, TL dating can not provide a resolution sufficient to differentiate short time intervals, which might be represented by such small differences. Therefore mean values from α-Al_2O_3:C-dosimetry (Table 2) are used for the external γ-dose-rate in calculating the ages for samples from the according layer and sub-layer. The internal dose rates ($D_{internal}$) were calculated after (Guerin et al., 2011) based on the Neutron Activation Analysis results (Table 1) for U, Th and K on 200 mg of sample material less than 160 μm from the extracted cores, which was obtained prior to the chemical treatment.

The dosemeters underestimate the cosmic dose rate before excavation because of the removal of several metres of sediment and the present day contribution was subtracted. Therefore the small cosmic dose contribution was estimated by taking into account the geographic position, altitude and estimated original thickness of sediments (Prescott and Stephan, 1982; Prescott and Hutton, 1994), employing a 5% uncertainty (after Barbouti and Rastin, 1983).

4.3. Results

4.3.1. Dosimetry results

The results of the Neutron Activation Analysis (Table 1) are rather variable as it is expected from the variety of raw materials used at the site, which originate probably from different geological sources. The samples EVA-LUM-05/21, -07/41 and -08/23 have unusual high K contents with large associated uncertainties. However, no systematics with NAA analysis could be discerned and the large analytical errors should cover most of the uncertainties which can not be accounted for (e.g. inhomogeneous distribution of K). In contrast, samples EVA-LUM-08/25 and -08/26, which were measured in a different batch, have very low radionuclide concentrations in general, but no systematic error in that analysis could be detected either. None of the measurements is therefore believed to be in error and no results are rejected.

HpPGe γ-spectrometry on the fine grained fraction of the sediment (<10 mm plus bone fragments of even larger size) does not indicate any disequilibrium in the ^{238}U- or Th-decay chain in

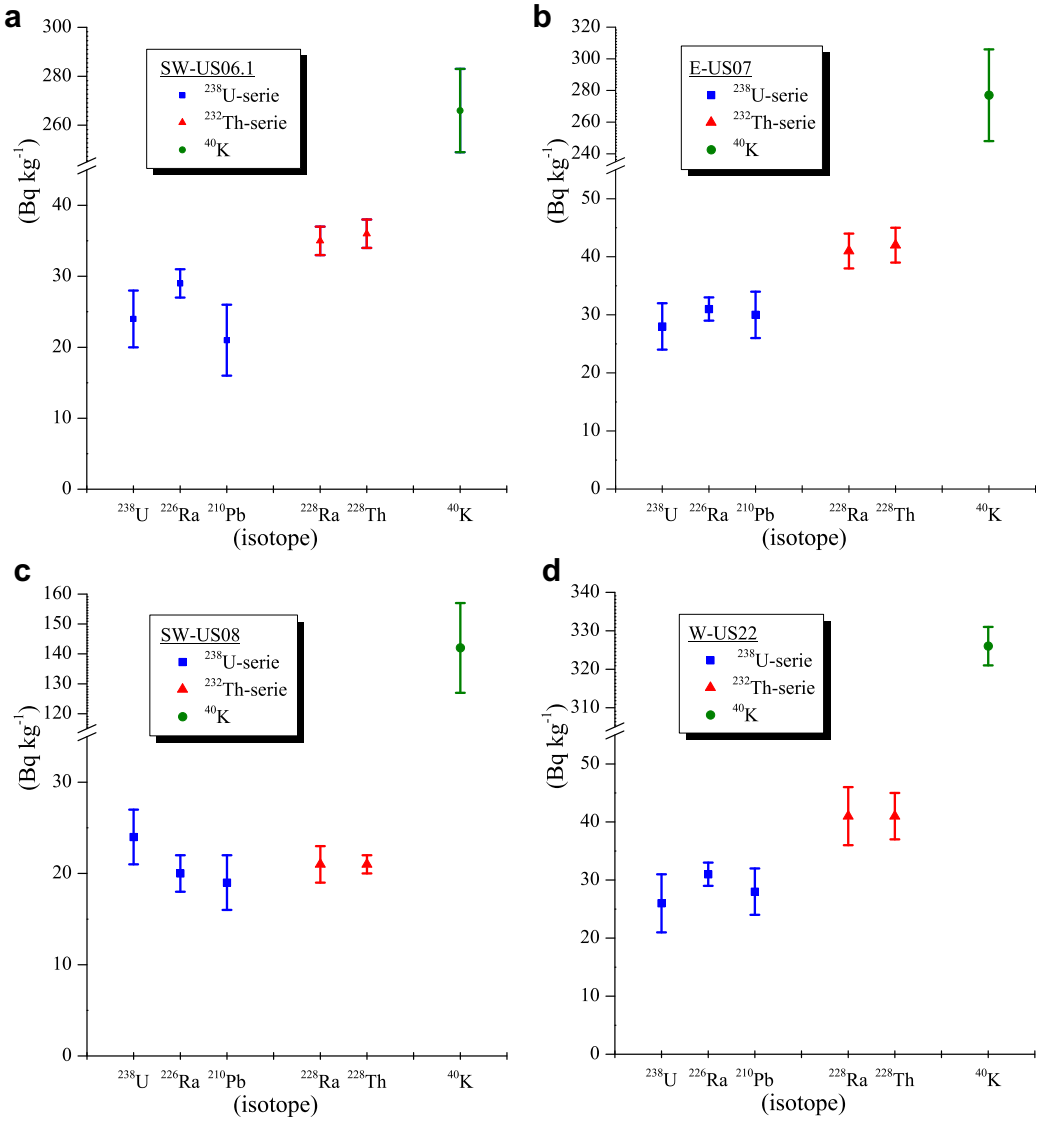

Fig. 4. Results (2-σ) of HpGe γ-ray spectrometry on dry sediment samples for a) layer SW-US6.1, b) layer E-US07, c) layer SW-US08 and d) layer W-US22.

any of the sediments (Fig. 4 & Table S-1) analysed. The external γ-dose rate was therefore assumed to have been constant over the entire burial time and the results of the α-Al_2O_3:C-dosemeters (Richter et al., 2010) measurements (Table 2) were used for age calculation. The attempt to place dosemeters in a large variety of geometries within the sediments, which are assumed to be very similar to the ones occupied by the samples, could be verified in this study, because some dosemeter locations were exposed by subsequent excavation. This allowed the verification of several dosemeter positions within the sedimentologically defined layers. Additionally, it was found that in fact geometries very similar to the ones for artefacts were measured, including such as some of the dosemeter having been situated (placed) in locations of rather loose sediment, small clay pockets as well as directly adjacent to rocks (e.g. dosemeter 35). All such types of geometries were observed for lithic artefacts in the site and thus for samples as well. Standard deviations up to 15% were obtained for the γ-dose rate for some layers (Table 2), while individual standard deviations of single dosemeters range between 3 and 10%. The variation of observed results correlates with the 'lumpiness' of the sediments and an associated uncertainty of 20% for the external γ-dose rate was used for all TL-dating. It is therefore assumed, that smaller variations during the entire burial due to changes which can not be accounted for (e.g. changes in moisture) are included.

Table 2
Locations and external γ-dose rates for α-Al_2O_3:C dosemeters and the mean for individual layers.

Dosemeter ID	Area/layer	Year	*x* (m)	*y* (m)	*z* (m)	μGy a^{-1}	Mean	sd (%)
10	E-US05.2	2005	1012.967	1087.184	−4.111	586		
11	E-US05.2	2005	1012.967	1086.360	−4.187	779		
12	E-US05.2	2005	1012.959	1085.462	−4.315	819		
13	E-US05.2	2005	1012.927	1084.617	−4.394	912		
	E-US05						**774**	**15**
191	E-US06.1	2007	1012.963	1087.402	−4.381	675		
192	E-US06.1	2007	1012.942	1086.583	−4.507	653		
199	E-US06.1	2007	1012.944	1085.904	−4.717	605		
	E-US06						**644**	**5**
3	E-US08	2004	1011.471	1089.399	−4.394	287		
4	E-US08	2004	1011.905	1087.434	−4.730	305		
	E-US08						**296**	**3**
18	SW-US05	2005	1005.586	1089.167	−3.671	365		
19	SW-US05	2005	1006.039	1090.454	−3.462	369		
	SW-US05						**367**	**1**
14	SW-US06	2005	1004.898	1081.820	−5.677	410		
15	SW-US06	2005	1004.139	1082.138	−5.398	403		
22	SW-US06	2005	1005.583	1088.936	−3.956	352		
	SW-US06						**388**	**7**
5	SW-US07	2004	1004.917	1084.888	−5.033	250		
6	SW-US07	2004	1005.755	1084.890	−5.145	297		
21	SW-US07	2005	1005.702	1088.735	−4.202	303		
24	SW-US07	2005	1005.898	1088.279	−4.481	244		
26	SW-US07	2005	1005.634	1089.022	−4.222	284		
35	SW-US07	2005	1005.802	1087.717	−4.439	334		
201	SW-US07	2007	1005.584	1085.506	−5.006	326		
206	SW-US07	2007	1005.583	1086.700	−4.727	275		
212	SW-US07	2007	1005.575	1088.969	−4.192	220		
	SW-US07						**281**	**13**
7	SW-US08	2004	1005.609	1084.858	−5.265	443		
8	SW-US08	2004	1006.204	1085.951	−5.068	303		
9	SW-US08	2004	1006.235	1086.555	−4.981	464		
16	SW-US08	2005	1005.002	1081.874	−5.899	474		
17	SW-US08	2005	1004.223	1082.198	−5.713	559		
20	SW-US08	2005	1005.878	1087.909	−4.697	266[a]		
23	SW-US08	2005	1005.769	1087.380	−4.698	405		
27	SW-US08	2005	1005.826	1088.098	−4.656	354		
213	SW-US08	2007	1004.221	1082.542	−5.705	469		
224	SW-US08	2007	1004.208	1083.192	−5.543	378		
225	SW-US08	2007	1004.223	1083.890	−5.352	436		
226	SW-US08	2007	1006.644	1081.752	−6.120	400		
228	SW-US08	2007	1006.248	1081.64	−6.055	405		
	SW-US08						**424**	**15**
28	SW-US09	2005	1006.111	1089.068	−4.613	611		
29	SW-US10	2005	1006.201	1088.341	−4.881	588		
1	W-US22AB	2004	1006.941	1091.183	−5.907	515		
2	W-US22AB	2004	1007.158	1091.289	−6.436	Failed		
30	W-US22AB	2005	1007.625	1092.171	−5.951	528		
31	W-US22AB	2005	1007.651	1091.495	−5.969	579		
33	W-US22AB	2005	1007.630	1091.688	−6.271	477		
32	W-US22AB1	2005	1007.614	1091.286	−5.993	575		
34	W-US22AB1	2005	1007.615	1091.328	−6.272	577		
	W-US22						**542**	**7**

[a] Value excluded because dosemeter was shallowly placed into a rock.

4.3.2. Thermoluminescence measurement results

A total of 74 flints showing signs of having been exposed to fire were tested for the sufficiency of the prehistoric heating with the heating plateau test (Aitken, 1985). 29 samples showed heating to >400 °C of the outer part of the samples, but only a total of 23 samples passed the test for the interior material of the sample as well (Table 1). This includes samples EVA-LUM-06/35, -06/36, -06/37 and -06/38. But the luminescence from these samples exhibits a peak at 220 °C, which was not present in the natural samples, and only slightly developed in the test measurements. It was assumed that any interference from this peak is negligible, because it occurs at a temperature about 150 °C lower than the peak (360–375 °C) employed for dating. However, it became of significant intensity for irradiated aliquots and showed 'abnormal' behaviour by growing at different rates for different aliquots, probably also independently of dose. Such differences in TL response might be related to the disproportional occurrence of materials with different luminescence behaviour on the different aliquots. Samples EVA-LUM-06/35 to -06/38 are therefore not suited for TL-analysis and were therefore rejected, because no reliable palaeodose can be deduced from such samples, of which the luminescence properties are currently investigated (Richter, forthcoming). No 'abnormal' behaviour was observed for the remaining 19 samples for which ages were calculated, with a triple age determination by identical procedures for sample EVA-LUM-07/42, which are independent except the fact that the sample material originates from different portions of a single lithic artefact.

The results of the luminescence measurements are reported with the ages (Table 3) and replace the preliminary TL-dating results previously reported (Jaubert et al., 2008).

The alpha efficiencies are quite variable and it is apparent from the repeat sample EVA-LUM-07/42, that the determination is not straight forward as evidenced by the variable results obtained, while all the other data for the three sub-samples is in excellent agreement. The ages agree as well, but only because of the low concentrations in radionuclides, which makes the internal dose rate less significant. These results indicate the need for improvement of the determination of the alpha sensitivity for samples where the internal contribution to the dose rate is dominant.

Overall, the ages are rather dependant on the assumption of constancy of the external γ-dose rate (Richter, 2007), and in fact, are also somewhat dependent on the estimation of the cosmic dose as well, because of the low external γ-dose rate in some cases, e.g. in layer SW-US07 (Table 3). In all cases the external γ-dose makes up more than 50% of the total dose-rate and the cosmic contribution up to about 30%.

The age results for the Quina Mousterian from Layer W-US22 range from 68 to 81 ka. Sample EVA-LUM-08/26 has an extremely low alpha sensitivity (Table 3). However, because of the very low content in radionuclides (Table 1) of this bright chalcedony-like sample the effect on the dose rate is small and the resulting age agrees very well with the estimates for the other two samples already at 1-σ (Table 3).

For the Denticulate Mousterian assemblage from Layer SW-US08 a total of eight samples were measured, giving ages between of 47.3 ± 7.1 ka and 66.0 ± 9.3 ka. The lowest age is

Table 3
Results of luminescence measurements and ages. An uncertainty of 5% was assumed for the cosmic dose-rate (after Barbouti and Rastin, 1983).

EVA-LUM-#	Area/layer	Palaeodose (Gy)	*b*-value (Gy μm^2)	$D_{\gamma-\text{ext. eff.}}$ (μGy a^{-1})	D_{cosm} (μGy a^{-1})	$D_{\alpha-\text{eff.}}$ (μGy a^{-1})	D_{β} (μGy a^{-1})	D_{total} (μGy a^{-1})	$D_{\gamma-\text{ext.}}$ (% D_{total})	D_{internal} (% D_{total})	Age (ka)
05/20	E-US05.2	59.8 ± 1.0	4.98 ± 0.12	704	150	52 ± 5	140 ± 24	1046 ± 143	67	18	57.1 ± 9.2
06/30	E-US05.2	26.9 ± 0.6	5.37 ± 0.15	735	150	50 ± 6	97 ± 8	1033 ± 148	71	14	26.0 ± 4.5
07/40	E-US05.2	87.6 ± 1.6	5.03 ± 0.07	697	150	94 ± 8	188 ± 43	1128 ± 146	62	25	77.6 ± 11.7
05/21	SW-US06.1	38.0 ± 0.8	4.49 ± 0.15	376	154	52 ± 9	337 ± 85	919 ± 114	41	42	41.3 ± 4.9
07/41	SW-US06.1	45.0 ± 1.5	3.94 ± 0.03	370	154	30 ± 4	98 ± 8	652 ± 75	57	20	69.1 ± 10.5
08/23	SW-US06.3	42.3 ± 1.2	3.41 ± 0.03	372	154	25 ± 4	94 ± 9	645 ± 75	58	18	65.6 ± 9.6
Simple mean	**SW-US06**										**58.7 ± 15.1**
07/42a	SW-US07	35.5 ± 1.4	4.84 ± 0.02	262	150	33 ± 4	79 ± 5	525 ± 53	50	21	67.6 ± 9.5
07/42b	SW-US07	33.7 ± 1.3	3.77 ± 0.04	254	150	26 ± 2	77 ± 5	507 ± 52	50	20	66.5 ± 9.2
07/42c	SW-US07	34.4 ± 1.6	2.65 ± 0.02	261	150	17 ± 2	75 ± 6	504 ± 53	52	18	68.3 ± 10.9
07/43	SW-US07	32.9 ± 0.6	0.94 ± 0.03	267	150	7 ± 0	87 ± 2	510 ± 54	52	18	64.5 ± 8.4
Weighted mean	**SW-US07**										**66.5 ± 5.2**
06/31	SW-US08	55.9 ± 1.8	0.99 ± 0.04	400	150	14 ± 2	282 ± 35	847 ± 88	47	35	66.0 ± 9.3
06/32	SW-US08	44.0 ± 1.3	1.23 ± 0.04	397	150	12 ± 0	138 ± 21	697 ± 82	57	22	63.1 ± 9.5
06/33	SW-US08	37.8 ± 1.2	1.23 ± 0.04	399	150	20 ± 2	230 ± 35	799 ± 88	50	31	47.3 ± 7.1
07/44	SW-US08	40.2 ± 1.3	1.06 ± 0.03	387	150	13 ± 1	126 ± 6	675 ± 78	57	20	59.5 ± 9.2
06/34	SW-US08	36.7 ± 1.1	1.30 ± 0.03	404	150	14 ± 1	122 ± 5	689 ± 81	59	20	53.2 ± 8.2
07/45	SW-US08	38.7 ± 1.0	0.95 ± 0.05	399	150	8 ± 1	103 ± 5	661 ± 80	60	17	58.6 ± 9.2
07/46	SW-US08	40.0 ± 1.5	1.00 ± 0.04	395	150	7 ± 1	130 ± 6	682 ± 80	58	20	58.6 ± 9.6
08/24	SW-US08	44.5 ± 1.1	0.57 ± 0.05	383	150	10 ± 1	176 ± 11	719 ± 78	53	26	62.0 ± 8.9
Weighted mean	**SW-US08**										**57.5 ± 3.5**
07/47	W-US22.1	59.4 ± 2.0	1.85 ± 0.03	518	133	27 ± 2	158 ± 6	835 ± 104	62	22	71.1 ± 11.6
08/25	W-US22	59.8 ± 2.5	0.56 ± 0.01	518	133	4 ± 1	81 ± 7	735 ± 104	70	12	81.3 ± 14.3
08/26	W-US22.2	46.5 ± 1.7	0.15 ± 0.01	525	133	1 ± 1	26 ± 15	684 ± 106	77	4	68.0 ± 12.7
Weighted mean	**W-US22**										**72.7 ± 7.9**

For the external γ-dose rate an uncertainty of 20% was assumed and corrected for shape and weight (after Valladas, 1985).

provided by a sample with a rather high K-content (EVA-LUM-06/33), but another sample with an even higher K-value (EVA-LUM-06/31) gave an age very similar to the other samples from this layer (Table 3). This is an indication that inhomogeneous K-distribution is not responsible for such a low age, but rather a result of the external γ-dose-rate value which had to be used.

Only two samples are available for the MTA Layer SW-US07, one of which (EVA-LUM-07/42) was split in 3 parts and treated as independent samples, including individual NAA analysis for all three parts. The resulting ages for this sample are identical at around 67 ka (Table 3) and, therefore, provide confidence in the procedures, despite the differences in the determination of the alpha sensitivity. The age for the other sample (EVA-LUM-07/43) agrees very well within uncertainties at 64.5 ± 8.4 ka. The low external γ-dose rate is reflected in the small palaeodose values for these samples, which ages all agree at 1-σ probability.

Two samples from Layer SW-US06, also MTA, give congruent results of 69.1 ± 10.5 ka and 65.6 ± 9.6 ka while another sample (EVA-LUM-05/21) provides a younger age of 41.3 ± 4.9 ka (Table 3) from this layer which is showing evidence of alterations.

The samples EVA-LUM-05/20, -06/30 and -07/40 from layer E-US05.2 give variable age results between 26 and 78 ka (Table 3) which confirms the archaeological interpretation of this layer as being mixed, which has already been suggested by geological/sedimentological analysis (Texier in Jaubert et al., 2008, p. 211). In this study samples from the same layer have rather different radionuclide contents, but nevertheless they provide congruent ages with the exception of samples from disturbed context. It is therefore not suspected that some NAA and alpha sensitivity measurements are in error and that the ages are not reliable. The samples from Layer W-US22 are very dependent on the external dose rate because of the low radionuclide concentrations. This results in large uncertainties for these samples because of a 20% uncertainty which was assumed for the external γ-dose rate for all samples.

5. Discussion of TL ages

The age results for Layer W-US22 pass the Shapiro–Wilk test at $p = 0.05$ (software package Origin 8.1), as well as a Chi-square test and, therefore, are considered to have been drawn from a normal population. The weighted mean is 72.7 ± 7.9 ka. The TL-dating results for Layer SW-US08 also belong to a normal distribution (Shapiro–Wilk and Chi-square passed). The statistical tests after Dixon (after Rorabacher, 1991) and Grubbs (Grubbs, 1969) for detecting outliers did not indicate the presence of outliers. A weighted mean age of 57.5 ± 3.5 ka is obtained for these samples. For Layer SW-US07 the weighted mean of the three age determinations on sub-samples of EVA-LUM-07/42 is 67.4 ± 6.2 ka, which is identical to the weighted mean of 66.5 ± 5.2 ka for all results under the assumption of independence. The latter might be a questionable assumption, but given the small sample number this is the best available age estimate for Layer SW-US07. It is obvious that more samples would be needed in order to provide a better age estimate for this layer and for Layer SW-US06. The three TL-dating results for layer SW-US06 do not belong to a normal distribution (Shapiro–Wilk and Chi-square failed at $p = 0.05$) and, therefore, only a mean age of 58.7 ± 15.1 ka can be given. However, the sample EVA-LUM-05/21 has an unusual high K-content, which might be responsible for its younger age if K is not distributed homogeneously (e.g. Schmidt et al., 2012) and if such a/several hot spots were sampled for NAA analysis. However, the *in situ* nature of this deposit has been questioned (Jaubert et al., 2008), because artefacts are not well preserved and display rounded and damaged edges. Furthermore, according to fabric analysis the sediment is a debris flow, while geological observations reveal runoff and solifluction pattern. Rejection of this sample would give an average age about 10 ka older, which is statistically not different to the average of all samples from this layer. However, because there is no distinct evidence for inhomogeneous K-distribution, the age results overlap at 2-σ and sample numbers for this layer are too low in order to

statistically determine outliers, the simple mean age of 58.7 ± 15.1 ka is preferred for this layer.

The dating results for layer E-US05.2 are not normally distributed and the individual ages are in the expected range for Upper and Middle Palaeolithic assemblages from this mixed layer (Jaubert et al., 2008). While the external dosimetry certainly has changed during burial history because of re-deposition, it is rather similar for the upper layers (Table 2). The effect of dosimetric changes are not quantifiable, but they were likely not very large in this case, and the ages might not be so erroneous as they appear at first. However, TL dating here provides clear evidence for a depositional disturbance of this layer, and shows, within limitations, that the method can be used as a tool to test the integrity of stratigraphies where the content of a layer can not be distinguished on typo-/techno-logical grounds. Such an approach has already been used by e.g. Debenham (1994) and it can be suspected to be the case in layer SW-US06 of Jonzac as well. However, the ages for Layer E-US05.2 have little significance for the chronostratigraphical placement of the site.

The age inversion of the mean ages for Layers SW-US06 to SW-US08 is apparent because all data overlap at a probability level of 95%. Such an apparent inversion could be a result of the low number of sample for Layers SW-US06 and SW-US07. None of the calculated means is significantly different from the other and therefore the sequential occurrence in the stratigraphy plays an important role in the interpretation of the data. For Jonzac it is therefore especially important to simultaneously consider the average ages of TL and the stratigraphic order ('archaeostratigraphy').

6. Conclusions

TL dating of heated flint confirms the mixing of Layer E-US05.2 and provides hints on the disturbed nature of Layer SW-US06. The TL ages Layer E-US05.2 provide rough age estimates for the broad placement in time of the observed different lithic components of this layer, which are clearly attributed to the Middle Palaeolithic and the Upper Palaeolithic. In this verifiable context, TL is shown here to be a valuable tool for the detection of the mixing of lithic assemblages, which can be important for sites where typological and technological pattern otherwise would not allow a differentiation. Several samples are required to obtain a good age estimate for an archaeological layer by TL dating of heated flint (Richter, 2007) in order to obtain sufficient accuracy and precision to place an assemblage into a climatostratigraphical framework. This could be achieved here only for the layer SW-US08 with a mean age estimate of 57.5 ± 3.5 ka, which, at 2-σ, places the occupation(s) responsible for the accumulation of this Denticulate Levallois assemblage into MIS 4 to MIS 3 (MIS after Lisiecki and Raymo, 2005). This age estimate, in which much confidence can be placed because of the comparable large number of samples, provides a chronometric anchor point for the sequence. According to the TL-data an identical MIS assignment is possible for the two overlying MTA layers (SW-US06 and SW-US07), whereas the underlying Mousterian of Quina Type assemblage from layer W-US22 is older and can be nominally placed in MIS 5b to MIS 4 (2-σ). Even though MIS 5b is a colder phase, the fauna from Layer W-US22 at Jonzac does not appear to be compatible and it is more likely that the Quina occupation of layer W-US22 took place in the colder climate of MIS 4. This particular attribution is often assumed for sites in South-West France (e.g. Delpech, 1996; Discamps et al., 2011; Jaubert et al., 2010). As a consequence, the subsequent occupations of Denticulate-Levallois and MTA should be placed at the beginning of MIS 3, as suggested by the faunal evidence. By combining the TL-dating results of the last heating of lithic artefacts with the ecological information obtained through the faunal remains, which are associated with the archaeology, it is possible to place the sequence of Jonzac into a generalized climatostratigraphic framework. An important result of this study is that Quina technology is not restricted to MIS 3, as some chronometric data analysis (Guibert et al., 2008) have suggested up to now. This finding is supported by TL-dating results at Pech-de-l'Aze IV, which also provide similarly old ages for a Quina assemblage there (Richter et al., 2012).

Acknowledgements

We would like to thank S. Albert (MPI-EVA, Leipzig, Germany) for her help in sample preparation and TL-measurements, and the Max-Planck-Society and the Ministry of Culture (DRAC-SRA Poitou-Charentes) for financial support or authorization. The Neutron Activation Analysis was performed by T. Schifer (Curt-Engelhorn-Zentrum Archäometrie gGmbH, Mannheim, Germany) and HpGe γ-spectrometry by D. Degering (Verein für Kernverfahrenstechnik und Analytik Rossendorf e.V., Dresden, Germany).

Appendix A. Supplementary data

Supplementary data related to this article can be found at http://dx.doi.org/10.1016/j.jas.2012.09.003.

References

Airvaux, J., Leveque, F., 2004. L'industrie de la couche 8. In: Airvaux, J. (Ed.), Le site paléolithique de Chez-Pinaud à Jonzac, Charente-Maritime. Premiers résultats: études sur la coupe gauche, pp. 37–47.
Airvaux, J., Soressi, M., 2005. Nouvelles observations sur le Moustérien final du site paléolithique de Chez-Pinaud à Jonzac. Préhistoire du Sud-Ouest 12, 163–174.
Airvaux, J., Beauval, C., Bouchet, J.-M., Bourdillat, V., Busson, S., Cochard, D., Demars, P.-Y., Karnay, G., Lenoir, M., Lévêque, F., Soressi, M., 2004. Le site paléolithique de Chez-Pinaud à Jonzac. In: Charente-Maritime. Premiers résultats: études sur la coupe gauche.
Airvaux, J., 2004. Echec provisoire pour deux methodes. In: Airvaux, J. (Ed.), Le site paléolithique de Chez-Pinaud à Jonzac, Charente-Maritime. Premiers résultats: études sur la coupe gauche, p. 99.
Aitken, M.J., 1985. Thermoluminescence Dating. Academic Press, London.
Aitken, M.J., 1998. An Introduction to Optical Dating. The Dating of Quaternary Sediments by the Use of Photon-stimulated Luminescence. Oxford University Press.
Barbouti, A.I., Rastin, B.C., 1983. A study of the absolute intensity of muons at sea level and under various thickness absorber. Journal of Physics G: Nuclear Physics 9, 1577–1595.
Botter-Jensen, L., McKeever, S.W.S., Wintle, A.G., 2003. Optically Stimulated Luminescence Dosimetry. Elsevier, Amsterdam.
Britton, K., Grimes, V., Niven, L., Steele, T.E., McPherron, S., Soressi, M., Kelly, T.E., Jaubert, J., Hublin, J.-J., Richards, M.P., 2011. Strontium isotope evidence for migration in late Pleistocene Rangifer: implications for Neanderthal hunting strategies at the Middle Palaeolithic site of Jonzac, France. Journal of Human Evolution 61, 176–185.
Dean, J.S., 1978. Independant dating in archaeological analysis. In: Schiffer, M.B. (Ed.), Advances in Archaeological Method and Theory. Academic Press, New York, pp. 223–255.
Debenham, N.C., 1994. A guide to TL dating flint assemblages. In: Ashton, N., David, A. (Eds.), Stories in Stone, pp. 4–6.
Delpech, F., 1996. L'environnement animal des Moustériens Quina du Périgord. Paléo 8, 31–46.
Discamps, E., Jaubert, J., Bachellerie, F., 2011. Human choices and environmental constraints: deciphering the variability of large game procurement from Mousterian to Aurignacian times (MIS 5–3) in southwestern France. Quaternary Science Reviews 30, 2755–2775.
Genty, D., Combourieu-Nebout, N., Peyron, O., Blamart, D., Wainer, K., Mansuri, F., Ghaleb, B., Isabello, L., Dormoy, I., von Grafenstein, U., Bonelli, S., Landais, A., Brauer, A., 2010. Isotopic characterization of rapid climatic events during OIS3 and OIS4 in Villars Cave stalagmites (SW-France) and correlation with Atlantic and Mediterranean pollen records. Quaternary Science Reviews 29, 2799–2820.
Grubbs, F.E., 1969. Procedures for detecting outlying observations in samples. Technometrics 11, 1–21.
Guerin, G., Mercier, N., Adamiec, G., 2011. Dose-rate conversion factors: update. Ancient TL 29, 5–8.
Guerin, G., 2012. Numerical simulations and modeling of dosimetric effects in Quaternary sediments: application to luminescence dating methods. Ancient TL 30, 30.

Guibert, P., Bechtel, F., Schvoerer, M., Müller, P., Balescu, S., 1998. A new method for gamma dose-rate estimation of heterogenous media in TL dating. Radiation Measurements 29, 561–572.

Guibert, P., Bechtel, F., Schvoerer, M., Rigaud, J.P., Simek, J.F., 1999. Datation par thermoluminescence de sédiments chauffés provenant d'une aire de combustion moustérienne (Grotte XVI, Cénac et St-Julien, Dordogne, France). Revue d'Archéométrie 23, 163–175.

Guibert, P., Bechtel, F., Bourguignon, L., Brenet, M., Couchoud, I., Delagnes, A., Delpech, F., Detrain, L., Duttine, M., Folgado, M., Jaubert, J., Lahaye, C., Lenoir, M., Maureille, B., Texier, J.-P., Turq, A., Vieillevigne, E., Villeneuve, G., 2008. Une base de données pour la chronologie du Paléolithique moyen dans le Sud-Ouest de la France. In: Jaubert, J., Bordes, J.-G., Ortega, I. (Eds.), Les sociétés du Paléolithique dans un Grand Sud-Ouest de la France: nouveaux gisements, nouveaux résultats, nouvelles méthodes. Société Préhistorique Française, Bordeaux, pp. 19–40.

Guiter, F., Andrieu-Ponel, V., de Beaulieu, J.-L., Cheddadi, R., Calvez, M., Ponel, P., Reille, M., Keller, T., Goeury, C., 2003. The last climatic cycles in Western Europe: a comparison between long continuous lacustrine sequences from France and other terrestrial records. Quaternary International 111, 59–74.

Jaubert, J., Hublin, J.-J., McPherron, S.P., Soressi, M., Bordes, J.-G., Claud, E., Cochard, D., Delagnes, A., Mallye, J.-B., Michel, A., Niclot, M., Niven, L., Park, S.-J., Rendu, W., Richards, M., Richter, D., Roussel, M., Steele, T.E., Texier, J.-P., Thiébaut, C., 2008. Paléolithique moyen récent et Paléolithique supérieur ancien à Jonzac (Charente-Maritime): Premiers résultats des campagnes 2004–2006. In: Jaubert, J., Bordes, J.-G., Ortega, I. (Eds.), Les sociétés du Paléolithique dans un Grand Sud-Ouest de la France: nouveaux gisements, nouveaux résultats, nouvelles méthodes. Société Préhistorique Française, Bordeaux, pp. 203–244.

Jaubert, J., Hublin, J.-J., McPherron, S., Soressi, M., 2010. Le gisement paléolithique de Chez Pinaud à Jonzac (Charente-Maritime). In: Buisson-Cattil, J., Primault, J. (Eds.), Préhistoire entre Vienne et Charente. Hommes et sociétés du Paléolithique, Association des Publications Chauvinoises, Villefranche-de-Rouergue, pp. 117–121.

Jaubert, J., Bordes, J.-G., Discamps, E., Gravina, B., 2011. A new look at the end of the Middle Palaeolithic sequence in southwestern France. In: Derevjanko, A.P., Shunkov, M.V. (Eds.), Characteristic Features of the Middle to Upper Paleolithic Transition in Eurasia. Institute of Archeology and Etnography SB RAS, Novosibirsk, pp. 102–115.

Lisiecki, L.E., Raymo, M.E., 2005. A Pliocene–Pleistocene stack of 57 globally distributed benthic ^{18}O records. Paleoceanography 20, 1–17.

McPherron, S.P., Talamo, S., Goldberg, P., Niven, L., Sandgathe, D., Richards, M.P., Richter, D., Turq, A., Dibble, H.L., 2012. Radiocarbon Dates for the Late Middle Paleolithic at Pech de l'Azé IV, France. Journal of Archaeological Science 39, 3436–3442.

Mellars, P.A., 1965. Sequence an development of Mousterian traditions in Southwestern France. Nature 205, 626–627.

Mellars, P.A., 1969. The chronology of Mousterian industries in the Périgord region of south-west France. Proceedings of the Prehistoric Society 35, 134–171.

Mellars, P.A., 1996. The Neanderthal Legacy: an Archaeological Perspective from Western Europe.

Mercier, N., Valladas, H., Joron, J.L., Reyss, J.L., Lévêque, F., Vandermeersch, B., 1991. Thermoluminescence dating of the late Neanderthal remains from Saint-Césaire. Nature 351, 737–739.

Niven, L., Steele, T., Rendu, W., Mallye, J.-B., McPherron, S.P., Soressi, M., Jaubert, J., Hublin, J.-J., 2012. Neandertal mobility and large-game hunting: the exploitation of reindeer during the Quina Mousterian at Chez-Pinaud Jonzac (Charente-Maritime, France). Journal of Human Evolution 63, 624–635.

Orombelli, G., Maggi, V., Delmonte, B., 2010. Quaternary stratigraphy and ice cores. Quaternary International 219, 55–65.

Prescott, J.R., Hutton, J.T., 1994. Cosmic ray contributions to dose rates for luminescence and ESR dating: large depths and long-term variations. Radiation Measurements 23, 497–500.

Prescott, J.R., Stephan, L.G., 1982. The contribution of cosmic radiation to the environmental dose for TL dating. Latitude, altitude and depth dependances, PACT. Revue du groupe européen d'études pour les techniques physiques, chimiques et mathématiques appliquées à l'archéologie 6, 17–25.

Richards, M.P., Taylor, G., Steele, T., McPherron, S.P., Soressi, M., Jaubert, J., Orschiedt, J., Mallye, J.B., Rendu, W., Hublin, J.J., 2008. Isotopic dietary analysis of a Neanderthal and associated fauna from the site of Jonzac (Charente-Maritime), France. Journal of Human Evolution 55, 179–185.

Richter, D., Dombrowski, H., Neumaier, S., Guibert, P., Zink, A.C., 2010. Environmental gamma dosimetry with OSL of α-Al_2O_3:C for in situ sediment measurements. Radiation Protection Dosimetry 141, 27–35.

Richter, D., Dibble, H., Goldberg, P., McPherron, S., Niven, L., Sandgathe, D., Talamo, S., Turq, A., 2012. The Late Middle Palaeolithic in Southwest France: new TL dates for the sequence of Pech de l'Azé IV. Quaternary International. http://dx.doi.org/10.1016/j.quaint.2012.05.028.

Richter, D., 2007. Advantages and limitations of thermoluminescence dating of heated flint from Paleolithic sites. Geoarchaeology 22, 671–683.

Richter, D. Investigations into the thermoluminescence of SiO_2-bearing, non-quartz materials. Journal of Luminescence, forthcoming.

Rorabacher, D.B., 1991. Statistical treatment for rejection of deviant values: critical values of Dixon's "Q" parameter and related subrange ratios at the 95% confidence level. Analytical Chemistry 63, 139–146.

Sanchez Goni, M.F., Turon, J.L., Eynaud, F., Shackleton, N.J., Cayre, O., 2000. Direct land/sea correlation of the Eemian, and its comparison with the Holocene: a high-resolution palynological record off the Iberian margin. Geologie en Mijnbouw/Netherlands Journal of Geosciences 79, 345–354.

Schmidt, C., Rufer, D., Preusser, F., Krbetschek, M., Hilgers, A., 2012. Assessment of radionuclide distribution in silex by autoradiography. Archaeometry. http://dx.doi.org/10.1111/j.1475-4754.2012.00690.x.

Schwarcz, H.P., 1994. Current challenges to ESR dating. Quaternary Science Reviews 13, 601–605.

Sier, M.J., Roebroeks, W., Bakels, C.C., Dekkers, M.J., Brühl, E., De Loecker, D., Gaudzinski-Windheuser, S., Hesse, N., Jagich, A., Kindler, L., Kuijper, W.J., Laurat, T., Mücher, H.J., Penkman, K.E.H., Richter, D., van Hinsbergen, D.J.J., 2011. Direct terrestrial-marine correlation demonstrates surprisingly late onset of the last interglacial in central Europe. Quaternary Research 75, 213–218.

Soressi, M., Jones, H.L., Rink, W.J., Maureille, B., Tillier, A.m., 2007. The Pech-de-l'Aze I Neandertal child: ESR, uranium-series, and AMS ^{14}C dating of its MTA type B context. Journal of Human Evolution 52, 455–466.

Szmidt, C.C., Normand, C., Burr, G.S., Hodgins, G.W.L., LaMotta, S., 2010. AMS ^{14}C dating the Protoaurignacian/Early Aurignacian of Isturitz, France. Implications for Neanderthal-modern human interaction and the timing of technical and cultural innovations in Europe. Journal of Archaeological Science 37, 758–768.

Valladas, H., 1985. Datation par la thermoluminescence de gisements moustériens du sud de la France. Université Pierre et Marie Curie Paris VI, Paris, p. 178.

Wagner, G.A., 1998. Age Determination of Young Rocks and Artifacts. Springer, Berlin.

Wintle, A.G., Aitken, M.J., 1977. Thermoluminescence dating of burnt flint: application to a Lower Palaeolithic site, Terra Amata. Archaeometry 19, 111–130.

Wohlfarth, B., Veres, D., Ampel, L., Lacourse, T., Blaauw, M., Preusser, F., Andrieu-Ponel, V., Keravis, D., Lallier-Verges, E., Bjorck, S., Davies, S.M., de Beaulieu, J.-L., Risberg, J., Hormes, A., Kasper, H.U., Possnert, G., Reille, M., Thouveny, N., Zander, A., 2008. Rapid ecosystem response to abrupt climate changes during the last glacial period in western Europe, 40–16 ka. Geology 36, 407–410.